

Comparison of the Brayton–Brayton Cycle with the Brayton–Diesel Cycle

Mateusz Mostowy*, Łukasz Szablowski*

Institute of Heat Engineering, Warsaw University of Technology, 21/25 Nowowiejska Street, 00-665 Warsaw, Poland

Abstract

This article is a comparative analysis of two systems: Brayton–Brayton and Brayton–Diesel. These two systems were both compared with a simple cycle of a gas turbine as a benchmark. The paper compares and contrasts the various advantages and disadvantages of the systems. The comparison with the simple cycle was made possible by having the same mass flow of air at the inlet of the gas turbine compressor for all analyzed cases (in the case of the Brayton–Brayton system—at the inlet of the compressor of the first gas turbine).

Compared to the simple cycle, the Brayton–Brayton cycle has greater power and the Brayton–Diesel less. In terms of efficiency both systems outperformed the simple cycle, with the Brayton–Diesel system achieving slightly better results than the Brayton–Brayton.

Keywords: Gas turbine; Brayton–Brayton; Brayton–Diesel

1. Introduction

This text deals with issues surrounding modification of a simple cycle gas turbine, in particular harnessing waste heat energy. Available literature contains a wealth of information about the simple cycle gas turbine combined with the steam cycle (Combined Cycle) [1], but there is little on other types of complex cycles. Sometimes it is economically unjustifiable to build an additional steam cycle, other times it is simply unfeasible for other reasons, such as space restraints on oil rigs. Then alternative solutions to the Combined Cycle—in the shape of other types of complex gas turbine cycles—should be explored. Examples of other complex cycles are: Brayton–Brayton, Brayton–Diesel, Brayton with fuel cells [2–5], Brayton combined with Organic Rankine Cycle. The methods for modeling fuel cells are described in [6–8] and some experimental studies in [9]. There is also a possibility to combine the Brayton cycle (microturbines) with the Stirling engine. Some information on the modeling and testing of Stirling engines can be found in [10–15].

Central to this paper is a comparative analysis of two methods: Brayton–Brayton cycle and the Brayton–Diesel cycle.

Determining which of these two cycles is better depends on the criteria selected. The two factors that generally domi-

nate when assessing a gas turbine with a regeneration system are:

- power output N , MW, or net shaft work N_j , kJ/kg,
- thermal efficiency η_c , %.

However, other factors can apply depending on the circumstances, such as the power ramp up rate, MW/minute, space requirement, m², and weight of the unit, t. This paper analyzes the cycles from the thermodynamic point of view, ignoring the space requirement, m², and weight of the unit, t. As the analysis was static, the ramp up rate, MW/minute, was ignored as well. Essentially, the most important factors from the economic point of view are generated power N , MW, and thermal efficiency η_c , %. Hence, when comparing the Brayton–Brayton and Brayton–Diesel cycles, the focus shall be on which has higher N , MW, (N_j , kJ/kg) and/or η_c , %.

The literature is a rich source of information on Brayton–Brayton cycles. Theoretical bases are included for example in [16]. Information about the industrial applications of the Brayton–Brayton cycle (the Air Bottoming Cycle) or about themselves are included in [17]. Information is scarce on industrial applications of Brayton–Diesel cycles, suggesting limited interest. The literature has multiple resources on piston expanders in the Diesel cycle. They are used for example in gas reduction stations for energy recovery [18].

The present research looked at the thermal efficiency η_c , %, and net shaft work N_j , kJ/kg, of the Brayton–Brayton and Brayton–Diesel cycles and investigated the influence of

*Corresponding author

Email addresses: mateuszmostowy@gmail.com (Mateusz Mostowy), lukasz.szablowski@itc.pw.edu.pl (Łukasz Szablowski)

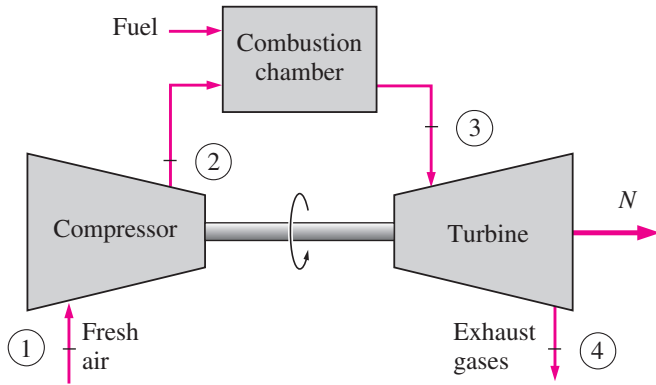


Figure 1: An open-cycle gas turbine engine (source: [19])

the parameters on the results in both cycles. Nowadays investors very rarely decide to build a simple cycle gas turbine out of concerns over efficiency and the environment. As fuel prices are a major issue, there is a drive to utilize to the greatest extent the energy available, including by adding heat recovery features to existing systems.

The comparative analysis determined which of the two cycles of interest is better and show advantages and disadvantages of the Brayton–Diesel cycle. The comparative analysis was facilitated by the fact that the cycles were a modification of the same simple cycle gas turbine.

2. Materials and Methods

In order to compare the Brayton–Brayton and the Brayton–Diesel cycle, both need to be modifications of the same simple cycle gas turbine. Modeling cycles with different boundary conditions would hamper any determination as to which cycle delivers a greater increase in efficiency and power.

2.1. Simple cycle (benchmark)

2.1.1. Thermodynamic description

The principle of the operation of a simple cycle gas turbine is based on the differences between the work used to compress fresh air in the compressor and the work obtained by the expansion of the exhaust gases in the turbine (Fig. 1). Fresh air at ambient parameters is compressed in the compressor, where its temperature and pressure rise. The air at high pressure then flows into the combustion chamber where combustion starts under constant pressure. Then hot exhaust gases expand in the turbine to ambient pressure. Power is generated on the shaft.

To generate power (net work W_{net}) on the shaft the work obtained in the turbine $W_{turbine}$ must be higher than the work used in the compressor $W_{compressor}$. This is shown in Fig. 2.

The thermodynamic cycle which describes the gas turbine engine is called the Brayton cycle after its inventor [19]. The cycle comprises four internally reversible processes:

- 1 → 2 Isentropic compression (in the compressor);

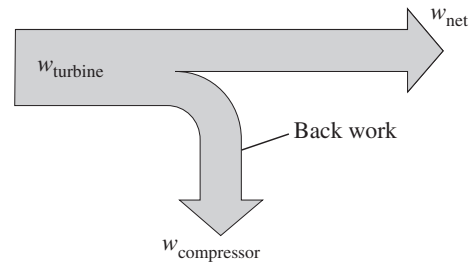


Figure 2: The fraction of the turbine work used to drive the compressor (source: [19])

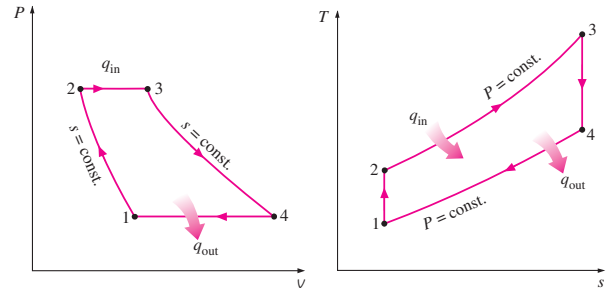


Figure 3: p-v and T-s diagrams for the Brayton cycle (source: [19])

- 2 → 3 Constant-pressure heat addition;
- 3 → 4 Isentropic expansion (in the turbine);
- 4 → 1 Constant-pressure heat rejection.

Processes occurring in the gas turbine, plotted on the p-v and T-s diagrams, were shown in the Fig. 3.

2.1.2. Calculation model

The entire system was modeled in the program HYSYS. The most commonly used fuel in the gas turbine engines is natural gas. Its composition is shown in Table 1.

Methane is the predominant constituent part of natural gas. To facilitate calculations, the fuel (p. 4 in Fig. 4) was modeled as 100% methane.

The fresh air (p. 1 in Fig. 4) used in all the processes in the cycle¹ was modeled in accordance with ISO conditions [21].

Fresh air relative humidity was obtained through appropriate molar proportion of individual factors at the inlet of the compressor (p. 1 in Fig. 4).

¹Should be noted that at the moment of “adding” fuel, the working medium is no longer the same air but is a mixture of air and fuel

Table 1: Composition of natural gas as a percentage of volume (source: [20])

gas	% of volume
CH ₄	98.39
C ₂ H ₆	0.44
C ₃ H ₈	0.16
C ₄ H ₁₀	0.07
C ₅ H ₁₂	0.03
N ₂	0.84
CO ₂	0.07

Table 2: ISO conditions for fresh air (source: [21])

ambient pressure	1.013 bar
ambient temperature	15°C
fresh air relative humidity	60%

Table 3: Molar proportion at the inlet of the compressor (p. 1 in Fig. 4) (source: own work)

components	molar proportions, %	mass proportions, %
water H ₂ O	1.01	0.6331
nitrogen N ₂	78.20	76.2194
oxygen O ₂	20.79	23.1475

The Peng-Robinson equation was used as the equation of state of the gas.

The parameters of individual system components are summarized in Table 4.

In order to obtain the characteristics of thermal efficiency η_c as a function of the pressure ratio Π pressure in point 2 (in Fig. 4) was changed in the next calculations. The range of changed values was: from 1.013 bar to 50 bar with step 0.1 bar. The characteristics of net shaft work N_j were obtained in a similar manner.

The simple cycle gas turbine model created in HYSYS was shown in Fig. 4.

2.2. Brayton–Brayton cycle

2.2.1. Thermodynamic description

The principle of operation of the Brayton–Brayton cycle is based on the use of exhaust heat from the simple cycle gas turbine. When the hot gases leave the gas turbine they are not released to the atmosphere but go instead to the heat exchanger. The heat exchanger works exactly like a combustion chamber for another gas (air) turbine. This way, more power is generated (but on two shafts) after burning the same amount of the fuel. The scheme of the Brayton–Brayton cycle is shown in Fig. 5.

The thermodynamic cycle which describes the Brayton–Brayton cycle consists of two Brayton cycles. The first—GT1—cycle was described in section 2.1.1 on page 98. The second—GT2—cycle comprises four internally reversible processes (as in GT1):

- 5 → 6 Isentropic compression (in the compressor);

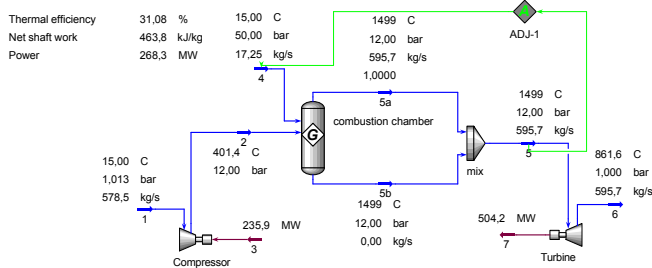


Figure 4: Simple cycle gas turbine modeled in HYSYS (source: own work)

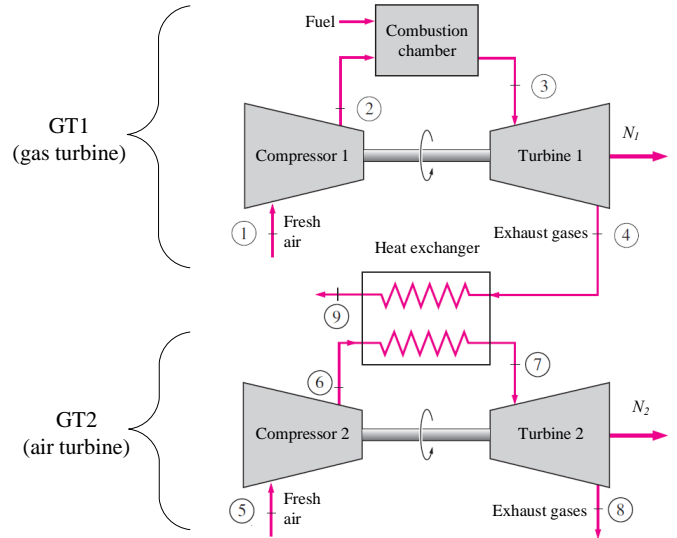


Figure 5: Scheme of the Brayton–Brayton cycle (source: based on the [19])

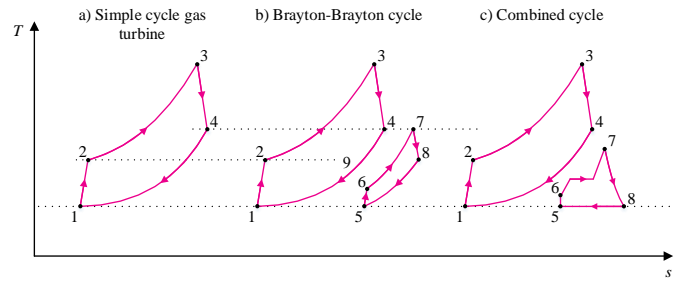


Figure 6: T-s diagrams for: a) Brayton cycle, b) Brayton–Brayton cycle, c) combined cycle (source: own work)

- 6 → 7 Constant-pressure heat addition;
- 7 → 8 Isentropic expansion (in the turbine);
- 8 → 5 Constant-pressure heat rejection.

Processes occurring in the Brayton–Brayton cycle plotted on the T-s diagram, were shown in Fig. 6 b).

2.2.2. Calculation model

The entire system was modeled in HYSYS software. The parameters of the fuel, fresh air and gas equation of state were as described in section 2.1.2 on page 98. Pressure, temperature, relative humidity, components of the fresh air in the bottom part of the Brayton–Brayton cycle were modeled in accordance with the ISO conditions [21] (like in the simple cycle).

This scheme consists of two Brayton cycles coupled together with the heat exchanger. The air part of the cycle (GT2 in Fig. 5) takes ambient air which is then heated in the heat exchanger (exhaust gases-fresh air). The heat exchanger was modeled so that it cools exhaust gases from the gas turbine (GT1 in Fig. 5) with a fixed temperature difference value equal to 100°C (difference between p. 4 and 7 in Fig. 5). Then the heated air expands in turbine 2.

Table 4: Parameters of individual system components in Fig. 4 (source: own work)

	no. on Fig. 4	pressure p , bar	temperature T , °C	mass flow \dot{m} , kg/s	efficiency, %
compressor—in	1	1.013	15	578.5	80
compressor—out	2	changed	—	—	—
fuel	4	50	15	changed	-
turbine—in	5	—	changed	—	80
turbine—out	6	1.013	—	—	—

efficiency was modeled as isentropic efficiency

compressor out pressure was changed after every calculation to get definite pressure ratio

turbine in temperature value was changed at 900°C, 1200°C, 1500°C

fuel mass flow was changed in such a way as to receive a certain temperature after the combustion chamber

Table 5: Reference parameters of the gas part in the Brayton–Brayton cycle (source: own work)

temperature T_3 , °C	optimal pressure ratio Π , -
900	9.8
1200	19.3
1500	35.8

In order to examine the possibility of applying the Brayton–Brayton cycle to increase the thermal efficiency of the simple cycle gas turbine, it was necessary to demonstrate the impact of various system variables. These variables were:

- pressure ratio of the compressor in the bottom part (air part) Π_{GT2} ;
- mass flow of the compressor in the bottom part (air part) \dot{m}_{GT2} .

The characteristics of the efficiency of the whole system as a function of the pressure ratio Π_{GT2} and the mass flow \dot{m}_{GT2} of the air part $\eta_c = f(\Pi_{GT2}, \dot{m}_{GT2})$ were designated for specific parameters of the gas part of the system (GT1 in Fig. 5). These parameters were:

- pressure ratio of the compressor in the gas part Π ;
- temperature after the combustion chamber T_3 (n. 3 in Fig. 5).

As reference parameters in the gas part, the optimal pressure ratios for 3 temperatures were chosen:

Parameters of individual system components are summarized in Table 6.

The Brayton–Brayton cycle model created in HYSYS was shown in Fig. 7.

2.3. Brayton–Diesel cycle

2.3.1. Thermodynamic description

The principle of operation of the Brayton–Diesel cycle is based partially on the use of the exhaust heat from the simple cycle gas turbine (as in the Brayton–Brayton cycle). This cycle consists of two different cycles:

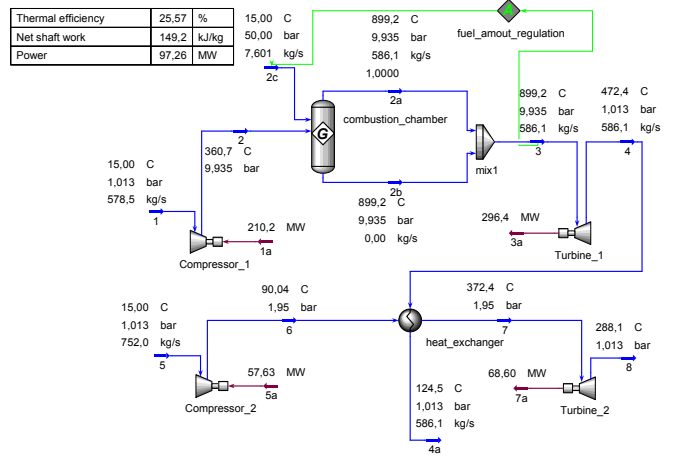


Figure 7: Brayton–Brayton cycle modeled in HYSYS (source: own work)

- Brayton cycle (as in gas turbines);
- Diesel cycle (as in cars).

When the hot gases leave the gas turbine they are not released to the atmosphere, but go to the heat exchanger. The heat exchanger warms part of the air from the compressor. After that the warmed air goes to the piston expander. In the piston expander power on the shaft is generated. After expansion, the air is not released directly to the atmosphere, but goes first to the turbine from the gas turbine cycle. After expanding in the turbine, the air is released to the atmosphere (once again through the heat exchanger). Noteworthy is that the Brayton–Diesel cycle is a combination of the turbo-machine and the piston-machine. A chart of the Brayton–Diesel cycle is shown in Fig. 8.

The thermodynamic cycle which describes the Brayton–Diesel cycle consists of two Brayton cycles. The gas turbine cycle was described in section 2.1.1. The Diesel cycle comprises four internally reversible processes:

- $1_D \rightarrow 2_D$ Isentropic compression (in a compressor);
- $2_D \rightarrow 3_D$ Constant-pressure heat addition;
- $3_D \rightarrow 4_D$ Isentropic expansion (in a turbine);

Table 6: Parameters of individual system components in Fig. 7 (source: own work)

	no. on the Fig. 7	pressure p , bar	temperature T , °C	mass flow \dot{m} , kg/s	efficiency, %
compressor 1—in	1	1.013	15	578.5	80
compressor 1—out	2	changed	—	—	—
fuel	2c	50.000	15	changed	—
turbine 1—in	3	—	changed	—	80
turbine 1—out	4	1.013	—	—	—
heat exchanger constant value $\Delta T = 100^\circ\text{C}$ (difference between T_4 and T_7)					
compressor 2—in	5	1.013	15	changed	80
compressor 2—out	6	changed	—	—	—
turbine 2—in	7	—	$T_4 - 100^\circ\text{C}$	—	80
turbine 2—out	8	1.013	—	—	—

efficiency was modeled as isentropic efficiency

compressor 1 out pressure was changed in accordance with Table 5

turbine 1 in temperature value was changed at 900°C, 1200°C, 1500°C

fuel mass flow was changed in such a way to receive a certain temperature after the combustion chamber

compressor 2 in mass flow was changed as 50%, 60%, 70%, 80%, 90%, 100%, 110%, 120%, 130% of the mass flow in compressor 1

compressor 2 out pressure value was changed in such a way to receive a pressure ratio of the air part Π_{GT2} from 2 to 10 with step 0.1

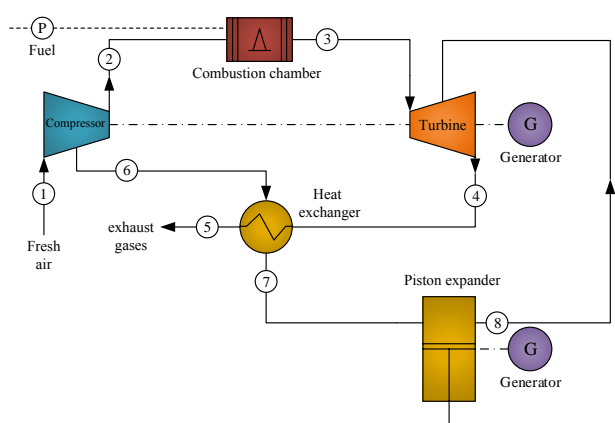


Figure 8: Scheme of the Brayton–Brayton cycle (source: own work)

- $4_D \rightarrow 1_D$ Constant-volume heat rejection.

The processes occurring in the Diesel cycle, plotted on the p-v and T-s diagrams, were shown in Fig. 9.

2.3.2. Calculation model

The entire system was modeled in the program HYSYS. The parameters of fuel, fresh air and the gas equation of state were described in subsection 2.1.2. This scheme consists of the Brayton cycle and the Diesel cycle coupled together with the heat exchanger. The Diesel part of the cycle (the piston expander in Fig. 8) takes compressed air which is then heated in the heat exchanger (exhaust gases-fresh air). The heat exchanger was modeled so as to cool exhaust gases from the gas turbine (Fig. 8) with a fixed recovery ratio of 0.85.

Recovery ratio:

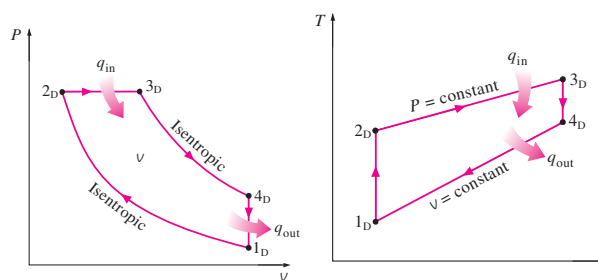


Figure 9: p-v and T-s diagrams for the Diesel cycle (source: [19])

$$\sigma = \frac{T_7 - T_6}{T_4 - T_6} \quad (1)$$

where: T_7 —temperature of the heated air after the heat exchanger, T_6 —temperature of the heated air after the compressor, T_4 —temperature of the exhaust gases after the turbine.

Then the heated air expands in the piston expander.

In order to examine the possibility of applying the Brayton–Diesel cycle to increase the thermal efficiency of the simple cycle gas turbine, it was necessary to demonstrate the impact of various system variables. These variables were:

- mass flow in the Diesel cycle \dot{m}_{2-D} ;
- pressure ratio in the Diesel cycle Π_D (compression ratio r).

As the reference parameters in the Diesel part, optimal pressure ratio for 1 temperature was chosen:

The parameters of individual system components are summarized in Table 8.

Brayton–Diesel cycle model created in HYSYS was shown on Fig. 10.

Table 7: Reference parameters of the Diesel part in the Brayton–Diesel cycle (source: own work)

temperature T_3 , °C	optimal pressure ratio Π_1 , –
1200	19.3

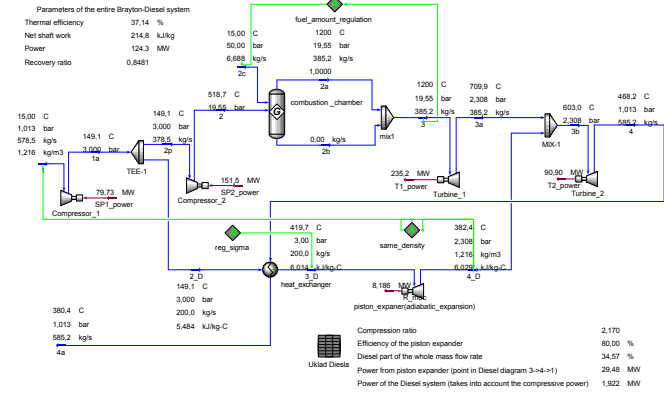


Figure 10: Brayton–Diesel cycle modeled in the program HYSYS (source: own work)

As it was not possible to model the piston expander in HYSYS, a spreadsheet package was used. Thermodynamic relationships which make possible to calculate the power and efficiency of the Diesel part were included in the spreadsheet. It then became possible to make the calculations. The thermodynamic relationships included in the spreadsheet are as follows:

- Power of the Diesel part:

$$N_D = N_{3D \rightarrow 4D} + N_{4D \rightarrow 1D} - N_{1D \rightarrow 2D} \quad (2)$$

where: $N_{3D \rightarrow 4D}$ —power obtained by the expansion of the piston expander, $N_{4D \rightarrow 1D}$ —power obtained by the constant-volume heat dissipation, $N_{1D \rightarrow 2D}$ —power consumed for the compression of the fresh air in the gas turbine compressor.

- Power obtained by the expansion of the piston expander $N_{3D \rightarrow 4D}$:

read from the program HYSYS (modeled as the expanding turbine)

- Power obtained by the constant-volume heat dissipation $N_{4D \rightarrow 1D}$:

$$N_{4D \rightarrow 1D} = \dot{m}_{2D} \cdot \rho^{-1} \cdot (p_{4D} - p_1) \quad (3)$$

where: \dot{m}_{2D} —the mass flow of the air to the Diesel part, ρ —density of the fresh air, p_i —the pressure in the point i .

- Power consumed for the compression of the fresh air in the gas turbine compressor $N_{1 \rightarrow 2}$:

$$\dot{L}_{1D \rightarrow 2D} = \dot{m}_{2D} \cdot (h_{2D} - h_1) \quad (4)$$

where: h_i —the enthalpy at point i .

The screenshot of the spreadsheet included in the Diesel part was shown in Fig. 11:

It must be noted that in all calculations only results that match the physical limitations were taken into account.

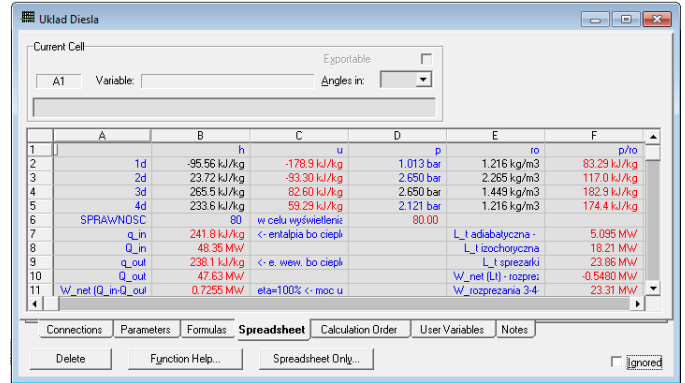


Figure 11: Brayton–Diesel cycle modeled in the program HYSYS (source: own work)

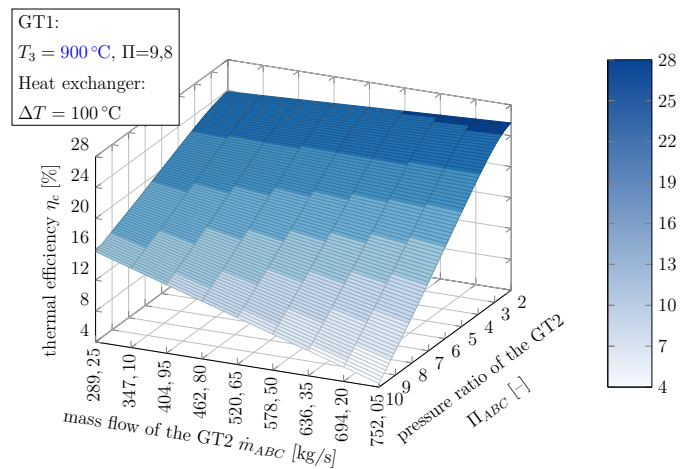


Figure 12: The thermal efficiency η_c of the Brayton–Brayton cycle for the temp. $T_3 = 900^\circ\text{C}$ (source: own work)

3. Results and discussion

3.1. Brayton–Brayton cycle

The thermal efficiency η_c of the Brayton–Brayton cycle as a function of the mass flow rate \dot{m}_{GT2} and pressure ratio Π_{GT2} of the bottom part $\eta_c = f(\Pi_{GT2}, \dot{m}_{GT2})$ are presented in Figures 12–14. The plot for the temperature $T_3 = 900^\circ\text{C}$ —Fig. 12.

Plot for the temperature $T_3 = 1200^\circ\text{C}$ —Fig. 13.

Plot for the temperature $T_3 = 1500^\circ\text{C}$ —Fig. 14.

As can be seen from Figures 12–14, determining the efficiency of the Brayton–Brayton involves a very complex relationship, combining many parameters of the two gas turbines.

These parameters are: temperature after the combustion chamber of GT1, pressure ratio in GT1, parameters of heat exchanger, pressure ratio in GT2, mass flow of air in GT2 (in relation to the mass flow in the GT1).

Thermal efficiency depends more strongly on the pressure ratio Π_{GT2} than on the mass flow \dot{m}_{GT2} . Power output in the Brayton–Brayton cycle is the sum of the power generated in the GT1 and GT2 part. The division of the power generated as a function of Π_{GT2} was shown in Fig. 15.

Table 8: Parameters of individual system components in Fig. 10 (source: own work)

	no. on Fig. 10	pressure p , bar	temperature T , °C	mass flow \dot{m} , kg/s	efficiency, %
compressor 1—in	1	1.013	15	578.5	80
compressor 1—out	1a	changed	—	—	—
compressor 2—in	2p	—	—	$\dot{m}_1 - \dot{m}_{2,D}$	80
compressor 2—out	2	19.550	—	—	—
fuel	2c	50	15	changed	—
turbine 1—in	3	—	1200	—	80
turbine 1—out	3a	$p_{4,D}$	—	—	—
turbine 2—in	3b	—	—	—	80
turbine 2—out	4	1.013	—	—	—
recovery ratio			$\sigma = \frac{T_{3,D} - T_{2,D}}{T_{4,D} - T_{2,D}} \approx 0,85$		
h. e.—in	2_D	changed	—	changed	—
h. e.—out	3_D	—	changed	—	—
piston—BDC	4_D	changed	—	—	—

Efficiency was modeled as isentropic efficiency, compressor 1 out pressure was changed after every calculation to obtain the specified pressure ratio, fuel mass flow was changed so as to receive a certain temperature after the combustion chamber, heat exchanger in the classic Diesel engine that will be the state before the fuel burns in the combustion chamber. In the analyzed model it is the inlet to the heat exchanger, heat exchanger in pressure value was changed to obtain the specified compression ratio of the Diesel part. The vales of the pressure: from 2.026 bar to 9.177 bar with step 0.1013 bar, heat exchanger in the mass flow the value of the mass flow in the Diesel part ranges from 10 kg/s to 350 kg/s, step 1 kg/s, heat exchanger out in the classic Diesel engine that will be the state after the combustion reaction in the combustion chamber ends. In the analyzed model that is inlet to the heat exchanger, heat exchanger out temperature the value was changed in such a way as to obtain the recovery ratio $\sigma = 0.85$ after every iteration, piston Bottom Dead Center piston/pistons in the piston expander are in Bottom Dead Center (after adiabatic expansion and before constant volume heat dissipation), piston Bottom Dead Center pressure was changed in such a way to get same specific volume at points 1 and 4_D

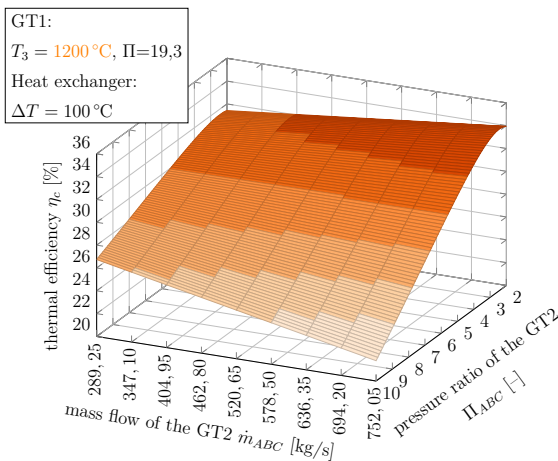


Figure 13: The thermal efficiency η_c of the Brayton–Brayton cycle for the temp. $T_3 = 1200^\circ\text{C}$ (source: own work)

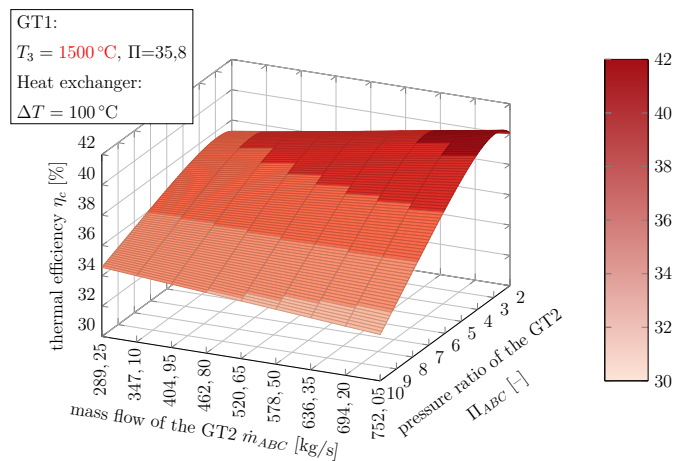


Figure 14: The thermal efficiency η_c of the Brayton–Brayton cycle for the temp. $T_3 = 1500^\circ\text{C}$ (source: own work)

3.2. Brayton–Diesel cycle

Power (and efficiency η_c) of the Brayton–Diesel cycle depends strongly on the mass flow rate $\dot{m}_{2,D}$ in the diesel part (Fig. 16) and on the pressure ratio Π_D in the diesel part (compression ratio r)—Fig. 17.

It is worth noting that both the mass flow rate $\dot{m}_{2,D}$ and the pressure ratio Π_D have a strong influence on the value of power generated in the Diesel cycle.

3.3. Summary

To make a meaningful assessment, the same conditions were adopted as with the base gas turbine system. These conditions were:

- mass flow rate $\dot{m}_1 = 578.5$ kg/s;

- temperature $T_3 = 1200^\circ\text{C}$.

The most efficient combinations of the variables were compared (Brayton-Brayton: \dot{m}_{GT2} , Π_{GT2} ; Brayton–Diesel: $\dot{m}_{2,D}$, Π_D).

The thermal efficiency of the analyzed cycles is shown in Fig. 18 and their power output in Fig. 19.

4. Conclusions

It is difficult to determine in absolute terms which of the systems presented in this paper is better. Much depends on the designated purpose for the system. Both the Brayton–Brayton cycle and Brayton–Diesel occupy a larger area than a conventional gas turbine system. This is due to the presence of a large heat exchanger, in which gases are the

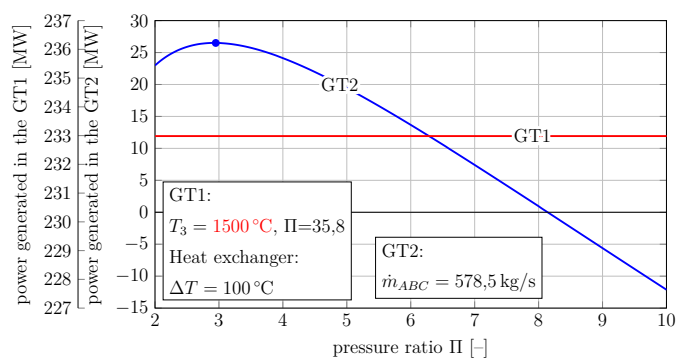


Figure 15: Power generated in the GT1 and GT2 as a function of Π_{GT2} (source: own work)

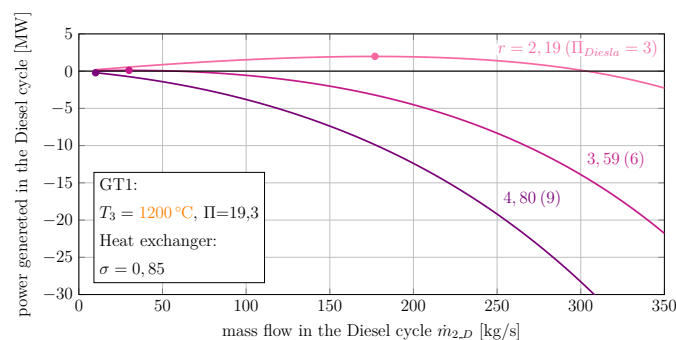


Figure 16: Power generated in the Diesel part as a function of the mass flow rate $\dot{m}_{2,D}$ (source: own work)

working fluid on both sides (which necessitates the considerable size). The Brayton–Brayton cycle has greater power than the simple cycle, and the Brayton–Diesel has less. Both systems outperformed the simple cycle in terms of efficiency, with the Brayton–Diesel system achieving slightly better results than the Brayton–Brayton. An interesting solution to increase the efficiency of the gas turbine is described in [22, 23].

References

- [1] K. Badyda, Perspektywy rozwoju technologii turbin gazowych oraz bloków gazowo-parowych, *Rynek Energii* 4 (113) (2014) 74–82.
- [2] J. Milewski, A. Miller, Off-design analysis of MCFC hybrid system, *Rynek Energii* 1.
- [3] J. Milewski, A. Miller, J. Sałaciński, Off-design analysis of sofc hybrid system, *International Journal of Hydrogen Energy* 32 (6) (2007) 687–698.
- [4] J. Milewski, T. Świercz, K. Badyda, A. Miller, A. Dmowski, P. Biczal, The control strategy for a molten carbonate fuel cell hybrid system, *international journal of hydrogen energy* 35 (7) (2010) 2997–3000.
- [5] J. Milewski, M. Wołowicz, R. Bernat, L. Szablowski, J. Lewandowski, Variant analysis of the structure and parameters of sofc hybrid systems, in: *Applied Mechanics and Materials*, Vol. 437, Trans Tech Publ, 2013, pp. 306–312.
- [6] J. Kupecki, J. Milewski, A. Szczesniak, R. Bernat, K. Motylinski, Dynamic numerical analysis of cross-, co-, and counter-current flow configuration of a 1 kw-class solid oxide fuel cell stack, *International Journal of Hydrogen Energy* 40 (45) (2015) 15834–15844.
- [7] J. Milewski, M. Wołowicz, A. Miller, R. Bernat, A reduced order model of molten carbonate fuel cell: A proposal, *International Journal of Hydrogen Energy* 38 (26) (2013) 11565–11575.

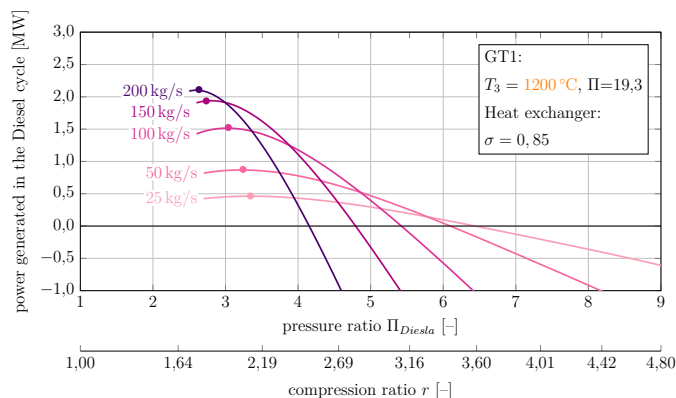


Figure 17: Power generated in the Diesel part as a function of the pressure ratio Π_D (compression ratio r) (source: own work)

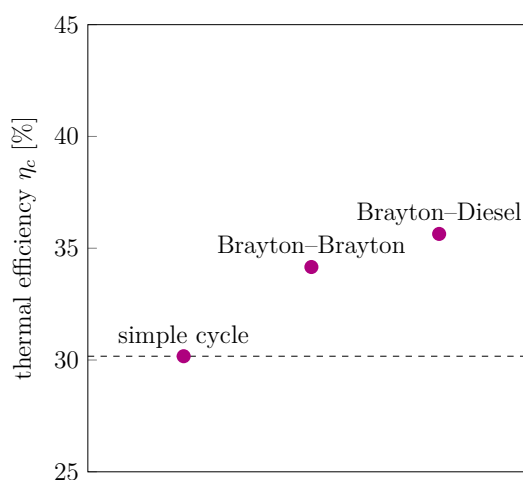


Figure 18: Thermal efficiency of the analyzed cycles (source: own work)

- [8] J. Milewski, K. Futyma, A. Szczesniak, Molten carbonate fuel cell operation under high concentrations of SO₂ on the cathode side, *INTERNATIONAL JOURNAL OF HYDROGEN ENERGY* 41 (41) (2016) 18769–18777, 3rd International Workshop on Molten Carbonates and Related Topics (IWMC), NE Univ, Shenyang, PEOPLES R CHINA, JUN 11-13, 2015. doi:10.1016/j.ijhydene.2016.03.121.
- [9] G. Cinti, U. Desideri, D. Penchini, G. Discepoli, Experimental analysis of sofc fuelled by ammonia, *FUEL CELLS* 14 (2) (2014) 221–230. doi:10.1002/uce.201300276.
- [10] D. Thombare, S. Verma, Technological development in the stirling cycle engines, *Renewable and Sustainable Energy Reviews* 12 (1) (2008) 1–38.
- [11] A. Chmielewski, R. Gumiński, S. Radkowski, Chosen properties of a dynamic model of crankshaft assembly with three degrees of freedom, in: *Methods and Models in Automation and Robotics (MMAR)*, 2015 20th International Conference on, IEEE, 2015, pp. 1038–1043.
- [12] A. Chmielewski, R. Gumiński, J. Mączak, S. Radkowski, P. Szulim, Aspects of balanced development of res and distributed microcogeneration use in poland: Case study of a μ chp with stirling engine, *Renewable and Sustainable Energy Reviews* 60 (2016) 930–952.
- [13] A. Chmielewski, S. Gontarz, R. Gumiński, J. Mączak, P. Szulim, Research study of the micro cogeneration system with automatic loading unit, in: *Challenges in Automation, Robotics and Measurement Techniques*, Springer, 2016, pp. 375–386.
- [14] K. Wang, S. R. Sanders, S. Dubey, F. H. Choo, F. Duan, Stirling cycle engines for recovering low and moderate temperature heat: A review, *Renewable and Sustainable Energy Reviews* 62 (2016) 89–108.
- [15] A. Chmielewski, S. Gontarz, R. Gumiński, J. Mączak, P. Szulim,

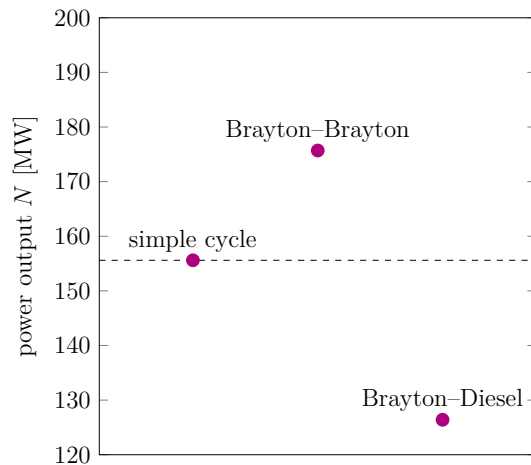


Figure 19: Power output of the analyzed cycles (source: own work)

Research on a micro cogeneration system with an automatic load-applying entity, in: *Challenges in Automation, Robotics and Measurement Techniques*, Springer, 2016, pp. 387–395.

- [16] K. Badyda, A. Miller, *Energetyczne turbiny gazowe oraz układy z ich wykorzystaniem*, Wydawnictwo Kaprint, 2014.
- [17] M. Korobitsyn, Industrial applications of the air bottoming cycle, *Energy Conversion and Management* 43 (9) (2002) 1311–1322. doi:10.1016/S0196-8904(02)00017-1.
- [18] Spilling Energie Systeme, Gas expansion. URL http://www.enesko.pl/images/Spilling-expander_prospekt.pdf
- [19] Y. Cengel, M. Boles, *Thermodynamics: An Engineering Approach with Student Resources DVD*, McGraw-Hill Education, 2010.
- [20] R. Kiš, M. Malcho, M. Janovcová, A CFD Analysis of Flow through a High-Pressure Natural Gas Pipeline with an Undeformed and Deformed Orifice Plate, *International Journal of Mechanical, Aerospace, Industrial, Mechatronic and Manufacturing Engineering* (2014) 606–609.
- [21] F. Brooks, GE Gas Turbine Performance Characteristics. URL <http://www.up.farsscript.ir/uploads/13316846411.pdf>
- [22] R. Szewalski, Sposób podwyższania sprawności obiegu energetycznego turbiny gazowej [a method of increasing the efficiency of the gas turbine's energy cycle] (1973).
- [23] P. Ziółkowski, M. Lemański, J. Badur, W. Zakrzewski, Wzrost sprawności turbiny gazowej przez zastosowanie idei szewalskiego, *Rynek Energii* (3) (2012) 63–70.